scientific reports

Check for updates

OPEN

Influence of conventional and sustainable electroless baths on autocatalytic copper deposition

Palanivelu Balaramesh[1,8], Raja Venkatesan[2,3]✉, Suseela Jayalakshmi[4], Munusamy Settu[5]✉, Eswaran Kamaraj[6,8], Alexandre A. Vetcher[7] & Seong-Cheol Kim[3]✉

This study compares the performance of commercial and eco-friendly electroless copper baths. Formaldehyde was used as a reducer in the commercial bath, and ethylenediaminetetraacetic acid (EDTA) as the chelating agent, and thiourea as the stabilizer, with potassium permanganate as a brightener and sodium hydroxide to maintain pH 13.0 at 60 °C. The environmentally friendly bath utilized potassium hydroxide to adjust the pH, polyol as the complexing agent, dimethylamine borane (DMAB) as a reducing agent, and biodegradable methanesulfonic acid (MSA) in trace quantities. In ideal circumstances (pH 11.0, 28 °C), benzotriazole (BTA, 1 ppm) had stabilizing effects. Atomic force microscopy (AFM), X-ray diffraction (XRD), and scanning electron microscopy (SEM) were used to study the coating's shape and structure. Its electrochemical behavior was simultaneously evaluated using Tafel polarization, electrochemical impedance spectroscopy (EIS), and cyclic voltammetry (CV). The commercial bath produced a higher deposition rate (2.72 µm h^{-1}) but yielded rougher surfaces (Ra ≈ 60 nm) with larger crystallites (25.55 nm). In contrast, the eco-friendly bath generated smoother, finer-grained deposits (Ra ≈ 21.62 nm; crystallite size = 17.82 nm) with uniform morphology. XRD confirmed the presence of crystalline copper in both systems. The eco-friendly bath showed excellent corrosion resistance in electrochemical testing, with a much lower corrosion current density and a greater charge-transfer resistance. Overall, the eco-friendly formulation delivered high-quality copper coatings with enhanced surface properties and corrosion resistance, while minimizing environmental impact.

Keywords Biodegradable, Brightener, Eco-friendly, Surface morphology, Xylitol

The choice between commercial and eco-friendly electroless baths plays a pivotal role in the autocatalytic copper deposition process. Commercial electroless baths typically contain various chemicals, including potentially hazardous or environmentally harmful substances. While effective in facilitating copper deposition, their usage raises concerns regarding environmental impact and safety[1–4]. On the other hand, eco-friendly electroless baths aim to mitigate these issues by employing less toxic or more biodegradable components. These baths promote sustainable practices and reduce environmental footprint without compromising deposition quality. However, the transition to eco-friendly alternatives may necessitate adjustments in deposition parameters to achieve comparable results. Overall, selecting the appropriate bath type involves balancing deposition efficiency with environmental considerations, thereby ensuring both technical efficacy and ecological responsibility in the copper deposition process[5–7].

Research on thin-film plating techniques has significantly increased in the last several years. Currently, metal finishing standards encompass 46 distinct processes, each comprising diverse technologies, operational procedures, inputs, and outcomes. Among these, electroless plating has attracted heightened interest due to its myriad advantages. Electroless plating permits the deposition of a noble metal from its salt solution onto the

[1]Department of Chemistry, R.M.K. Engineering College, Chennai, Tamil Nadu 601206, India. [2]Department of Biomaterials, Saveetha Dental College and Hospitals, SIMATS, Saveetha University, Chennai, Tamil Nadu 600077, India. [3]School of Chemical Engineering, Yeungnam University, 280 Daehak–Ro, Gyeongsan 38541, Republic of Korea. [4]Department of Chemistry, School of Basic Sciences, VISTAS, Pallavaram, Chennai, Tamil Nadu 600117, India. [5]Centre for Applied Nanomaterials, Chennai Institute of Technology, Chennai, Tamil Nadu 600069, India. [6]Department of Chemistry, Yeungnam University, 280 Daehak-Ro, Gyeongsan 38541, Republic of Korea. [7]Institute of Pharmacy and Biotechnology (IPhB), RUDN University n.a. P. Lumumba (RUDN), 6 Miklukho-Maklaya Str, Moscow 117198, Russian Federation. [8]Palanivelu Balaramesh and Eswaran Kamaraj contributed equally to this work. ✉email: rajavenki101@gmail.com; munu.tvm@gmail.com; sckim07@ynu.ac.kr

catalytically active surface of a less noble metal by using an appropriate reducing agent and functioning without the use of electrical energy. When the metallic ion is reduced by the reducing agent, a homogeneous, thin coating is created to cover the substrate surface[8–11].

The auto-catalytic process has enhanced the functionality of integrated circuits and circuit boards. Recent studies have explored various methods for the electroless deposition of metals, resulting in significant advancements in robotics and artificial intelligence domains[12–15]. In the late 20th century, substantial investments were made globally in nanotechnology research projects, emphasizing sensors, electronics, and energy conversion devices. Currently, both soft and hard gold-coated substrates are integral to the digital industry for manufacturing printed circuit boards (PCBs) and metallizing circuits and bonding semiconductor chips. Additionally, in the microelectronics domain, metallizing non-conducting polymer substrates offers numerous advantages[16–18].

Copper is now the material of choice for connecting expensive computer chips with information storage devices due to its greater electrical conductivity and improved resistance to electromigration; this position is anticipated to remain for some time to come. Basic surfaces for metals may be effectively protected against corrosion with electroless metal protective coatings. Electroless metal protection coatings are an efficient way to prevent corrosion on the metallic substrates[19–21]. Copper's inherent resistance to various liquids and atmospheric conditions ensures low porosity and reliable corrosion resistance. These coatings serve as an excellent base for subsequent layers, boasting uniform thickness, high hardness, exceptional resistance to wear and abrasion, absorbent properties, and strong adhesion[22–24].

Formaldehyde serves as a reducing agent in the predominant commercial electroless copper bath, prized for its affordability, effectiveness, and ease of regulation. Dimethylamine borane has emerged as a crucial reducing agent in electroless deposition applications, offering notable advantages such as high solubility, minimal toxicity, precise deposition rates, superior conductivity, and exceptional resistance to corrosion during deposit formation[25–27]. The study centers on the preparation of electroless baths utilizing formaldehyde with EDTA and DMAB with xylitol. A further novel feature of this study is the use of methanesulfonic acid (MSA), a biodegradable Bronsted acid, as the bath solution. Additionally, the environmentally benign bath is infused with trace amounts of chemicals, such as brightener and leveler, at a level of one part per million. While these additives do not affect the deposition rate, they do alter surface morphologies and improve the quality of the copper deposits.

Formaldehyde is the traditionally used reducing agent in the electroless plating process. When we use formaldehyde, the following two half-reactions take place in the electroless bath.

Cathodic reaction,

$$Cu^{2+} + 2e^{-} \rightarrow Cu$$

Anodic reaction,

$$2HCHO + 4OH^{-} \rightarrow 2HCOO^{-} + H_2\uparrow + 2H_2O + 2e^{-}$$

DMAB bath is less understood. In alkaline solution, DMAB gets easily dissociated with the formation of an intermediate hydroxytrihydroborate anion, which gets oxidized with the evolution of hydrogen gas. The two half-reactions taking place in a DMAB used in an electroless deposition bath are,

Cathodic reaction,

$$Cu^{2+} + 2e^{-} \rightarrow Cu$$

Anodic reaction,

$$(CH_3)_2NH.BH_3 + OH^{-} \rightarrow BH_3OH^{-} + (CH_3)_2NH$$

$$BH_3OH^{-} + 3OH^{-} \rightarrow B(OH)_4^{-} + 3H_2 + 3e^{-}$$

A critical factor in electroless copper deposition is the choice of reducing agent, as it governs coating quality, bath stability, cost, and environmental impact. Formaldehyde remains the most widely used option owing to its low cost and efficiency; however, its high toxicity and stringent environmental regulations have restricted broader application. Alternatives such as dimethylamine borane (DMAB) provide safer handling and yield smooth, corrosion-resistant coatings, but their higher cost and limited bath stability hinder large-scale use. More recently, biodegradable candidates such as xylitol and methanesulfonic acid (MSA) have attracted attention for their environmental compatibility, though they typically require careful optimization of bath chemistry to achieve performance comparable to traditional systems[30–32]. Reports in the literature indicate that conventional EDTA-formaldehyde baths often produce rougher surface morphologies and higher corrosion rates, largely due to their aggressive chemical environment. In contrast, eco-friendly baths employing organic reducing agents and stabilizers (e.g., glyoxylic acid, xylitol) have demonstrated smoother deposits with reduced toxicity. Nevertheless, systematic, side-by-side evaluations of commercial and eco-friendly formulations under identical conditions are still scarce, motivating the present study.

Materials and methods

Materials

Without additional purification, the chemical compounds were used after being sourced from the designated sources. Formaldehyde (Sigma-Aldrich), ethanol, sodium hydroxide (Sigma-Aldrich), ammonia (Fisher), copper methane sulphonates (S.D. Fine Chemicals), copper carbonate (Merck), xylitol (Fisher), EDTA (Sigma-Aldrich), and dimethylamine borane (DMAB) (Merck). All of the stock solutions were made with double-distilled water.

Experimental

A 1000 mL beaker was filled with around 100 g of weighed copper carbonate. Add 120 milliliters of methanesulfonic acid up to the point where carbon dioxide begins to evolve. Fill a standard volumetric flask with 500 mL of the solution using double-distilled water. After filtering out any obvious contaminants, the solution is stored. One millilitre of the stock solution will be mixed with a normal sodium thiosulfate solution (1:10), and copper will then be deposited. The quantity of copper in the stock solution is determined by the weight of the copper deposit. The stock solution preparation flowchart is shown below.

Autocatalytic copper deposition was carried out in a 100-milliliter beaker using epoxy sheets as the foundation material, as shown in Table 1. The base material was cleaned with twice-distilled water and polished with ultra-fine-grit sandpaper before usage. A solution of $KMnO_4$ and H_2SO_4 was used to etch the surface of the base material, and a solution of $SnCl_2$ was used to sensitize it. To activate the surface, a $PdCl_2$ solution in HCl was used.

In conventional activation using $PdCl_2 + HCl$, palladium ions (Pd^{2+}) are reduced to Pd^0 nuclei that act as catalytic for autocatalytic deposition, while copper at the surface undergoes partial oxidation. This redox exchange alters the initial copper surface state, increasing interfacial roughness and influencing nucleation density. Such modification can contribute to less uniform deposit morphology. By contrast, the eco-friendly xylitol/DMAB system reduces the extent of oxidative surface changes, thereby promoting smoother and more uniform copper nucleation.

Flow chart for the pretreatment of the substrate surface.

Specimen
↓ ← NaOH
Scouring
↓ ← Distilled water
Rinsing
↓ ← $KMnO_4 + H_2SO_4$
Etching
↓ ← $SnCl_2 + HCl$
Sensitization
↓ ← $PdCl_2 + HCl$
Activation
↓ ← Copper bath
Plating

Finding the copper rate for deposition

The following relation was used to determine the rate of deposition (T):

$$Deposition\ rate\ (\mu m/h)\, T = W \times 10^{-4}/dAt$$

Wherein A is the area of the covered layer (cm^3), t is the deposit's duration (h), d is the copper density (8.96 g cm^{-3}), and W is the mass of the coating (g).

Reducing agents/additives	Advantages	Limitations
Formaldehyde	Cheap, effective, reliable coatings	Toxic, carcinogenic, and disposal issues
DMAB	Smooth coatings, corrosion-resistant	Costly, stability issues, H_2 release
Xylitol	Eco-friendly, biodegradable	Slower kinetics, needs optimization
MSA	Low-toxicity, biodegradable medium	Less studied, bath needs additives

Table 1. Comparison of major reducing agents and additives for electroless copper deposition.

The rate of electroless copper deposition was determined using the equation:

$$Deposition\ rate\ \ (\mu m/h)\ \ =\ \ Thickness\,(\mu m)\,/Time\ \ (h)$$

Each measurement was performed in triplicate for reliability.

X-ray diffraction (XRD) analysis of phase composition

X-ray diffraction is used to investigate the morphological characteristics of the coated metallic copper during the autocatalytic coating technique studies using the X'Pert-Pro system from p-analytical. The sample is exposed to monochromatic collimated X-rays produced by a cathode ray tube. Because of the random nature of the material, the diffracted rays are able to record all potential lattice orientations when the sample is scanned across a range of 2θ angles. Following the conversion of these diffraction peaks into d-spacings, important information about the properties of the material is revealed. We use the Debye-Scherrer equation to calculate the particle size of the deposits.

$$D\ =\ K\ \lambda\ /\beta_{rad}\cos\theta$$

"K" stands for the Scherrer shape factor in the Debye-Scherrer equation, "λ" for the incoming radiation's wavelength for diffraction, "βrad" for the Full Width at Half Maximum (FWHM), well-defined peak in radians, and "θ" for the observed diffraction angle. The particle form is taken into consideration by the Scherrer shape factor (K), which is usually given a value of 0.89.

Assessing quantity as well as quality using cyclic voltage measurement (CV)

Using a conventional redox detector, periodic voltammetry profiles are obtained. Nitrogen gas deaerates the copper methane sulphonate mixture. A platinum wire served as the experiment's opposing electrode, while silver/silver chloride packed with a potassium chloride solution served as the reference electrode. An electrolyte with 0.1 M sodium sulphate and an ambient temperature of 28 ± 2 °C was used to construct voltage graphs. At a practical sweep rate of 50 mV/s, voltage graphs with a range of -1.2 to + 0.5 V were produced using a standard clear carbon electrode as the working electrode.

Direct current (DC), tafel polarization technique

An electrochemical approach was used to identify current responses that were collected when potentials that were sufficiently displaced from the corrosion potential were applied against the saturated calomel electrode (SCE) to create polarization plots for both the oxidative and reductive operations.

By plotting the logarithm of current density (log I) against corrosion potential and projecting the linear regions of the anodic and cathodic branches, polarization curves were obtained. These plots provide insights into the reduction current of copper salts, which is analogous to the oxidation current of glyoxylic acid. The corrosion rate was computed using Faraday's equation in the appropriate measurements based on the degree of corrosion density of the current (I_{corr}). Stern, along with Geary's revolutionary research, serves as the foundation for this approach and is being used today to measure corrosion rates.

The experiment's specific reference electrode was silver/silver chloride filled with a potassium chloride solution, and the opposing electrode was a platinum wire. Voltage graphs were created in an electrolyte containing 0.1 M sodium sulfate at an ambient temperature of 28 ± 2 °C. A conventional transparent carbon electrode was used as the working electrode, and voltage graphs with a range of -1.2 to + 0.5 V were recorded at a feasible sweep rate of 50 mV/s.

Electrochemical polarization measurements and impedance spectroscopy (EIS)

The EIS analysis is a valuable method for studying the corrosion behavior of an electroless bath. This technique is highly effective in characterizing metal-coated surfaces. A potential is passed between an active electrode and a counterpart electrode, and the resulting potential drop at the active electrode-electrolyte interface is closely monitored. Electrochemical impedance spectroscopy (EIS) measurements involve applying a small voltage, typically ranging from 5 to 50 mV, to a sample while scanning frequencies from 50 kHz to 10 mHz. The impedance response is recorded, capturing both its real and imaginary components. Analysing the Nyquist and Bode plots' shapes and fitting them to a comparable electrical circuit model allowed for the interpretation of the electrochemical impedance spectroscopy, EIS data. Quantitative information on the copper coatings' ability to withstand corrosion was obtained from the retrieved circuit characteristics (such as charge transfer resistance and double-layer capacitance).

Results and discussion

The elevated points at the (111), (200), and (220) planes were examined to assess the morphological characteristics of copper occurrences. In its face-cantered cubic arrangement, copper usually shows a more favourable position along the (111) axis, as seen in Fig. 1. The (111) orientation has become less important in our work due to the combined impact of enhanced conductivity and the soluble nature of prolonged methanesulfonic acid.

The inhibitory or accelerating effects of the stabilizers were compared to the deposition rate (μm/h) of the electroless plating plain bath. Stabilizers were deemed inhibitors if the deposition rates were lower than those of the plain bath, whereas they were considered accelerators or enhancers if the rates were higher. BTA exhibited higher values than the xylitol plain bath; however, thiourea showed a lower deposition rate than the EDTA plain bath. Both the electrochemical Tafel polarization method and the physical weight-gain approach were used to calculate the deposition coating rates.

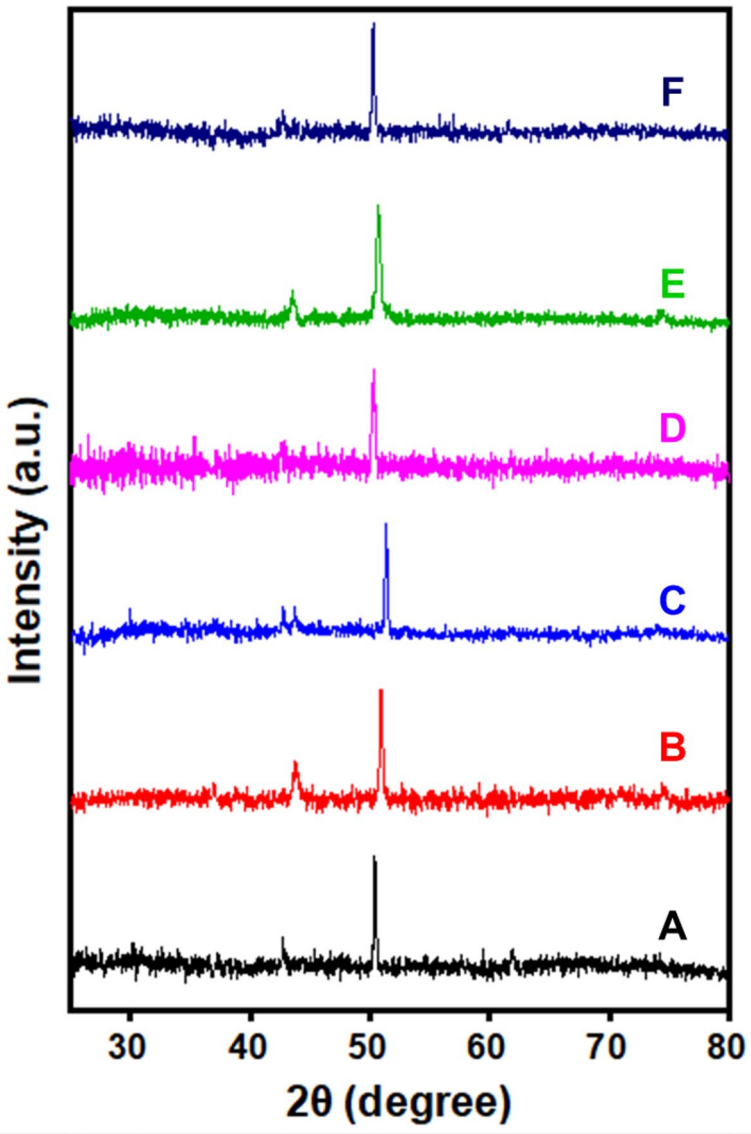

Fig. 1. (**A**) EDTA standard bath, (**B**) EDTA standard bath with thiourea, (**C**) EDTA standard bath in thiourea, along with $KMnO_4$ (1 ppm), (**D**) xylitol standard bath, (**E**) xylitol standard bath with MSA and BTA (1 ppm), and (**F**) xylitol standard bath with MSA and BTA (1 ppm) are copper-containing EDTA and xylitol contained methane sulphonate baths.

SEM analysis was used to examine the deposited copper's two-dimensional structure. SEM was used to examine the surface morphology of copper deposits on specimens used in additive and plain baths at a magnification of x 5000. When the dopant was added to the polyol bath, consistent, ultrafine copper deposits were formed, as seen in Fig. 2. To change the morphological characteristics of the copper deposits, including their geometry, hues, and lattice size, a small quantity of brightener and leveller is introduced.

This stabilizes the bath (Table 2). Various intriguing forms were observed, including grains, flowers, rocks, needles, and pyramids. Baths containing MSA and BTA exhibited floral patterns and smaller grains. The results indicate that, in contrast to the xylitol standard bath, the xylitol bath alters the physical properties of the layers of copper and develops a uniform, glossy surface.

Copper deposits observed through AFM with a bright appearance indicate high-quality mechanical and physical characteristics (Fig. 3). There exists an inverse relationship between smooth deposition and roughness values. Differences are found when roughness values are compared between the basic xylitol bath and baths containing stabilizers. At 76.017 nm, the roughness value is maximum in the EDTA plain bath. However, because stabilizers have steric effects, they reduce roughness. The roughness of the xylitol-based electroless bath is around 49.583 nm (Table 3). The use of brighteners and additives considerably changes the coarse silhouette.

Six sets of electrochemical data were examined to assess the properties of copper deposits obtained from commercial and eco-friendly electroless baths.

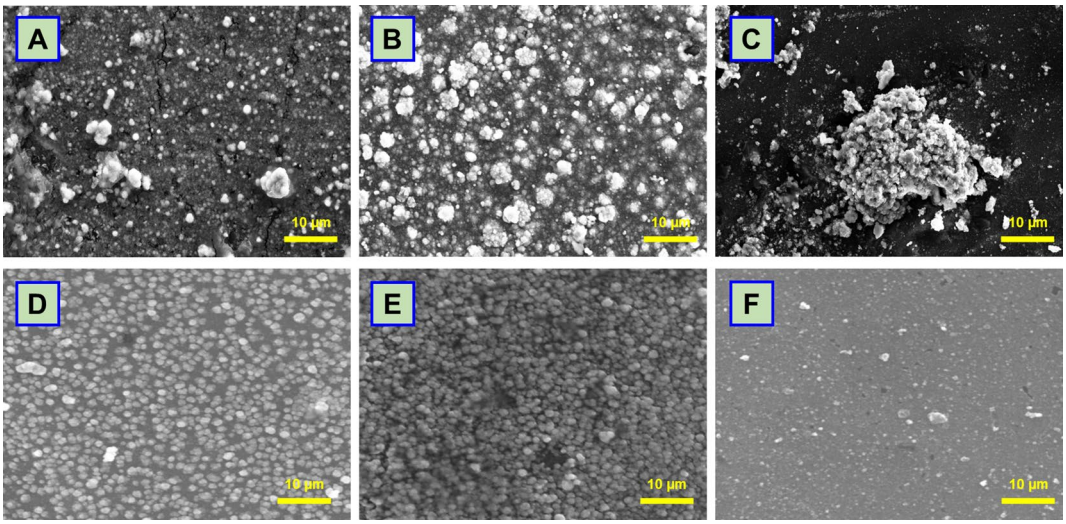

Fig. 2. SEM micrographs of copper films deposited from EDTA- and xylitol-based baths: (**A**) EDTA standard bath, (**B**) EDTA standard bath with thiourea, (**C**) EDTA standard bath in thiourea, along with $KMnO_4$ (1 ppm), (**D**) xylitol standard bath, (**E**) xylitol standard bath with MSA and BTA (1 ppm), and (**F**) xylitol standard bath with MSA and BTA (1 ppm).

Bath contains	EDTA plain bath	EDTA bath with stabilizer	EDTA bath with stabilizer and additives	Bath contains	Xylitol plain bath	Xylitol bath with stabilizer	Xylitol bath with stabilizer and additives
Cu ion contacting salt	3 g/L	3 g/L	3 g/L	Cu ion contacting salt	3 g/L	3 g/L	3 g/L
EDTA	20 g/L	20 g/L	20 g/L	Xylitol	20 g/L	20 g/L	20 g/L
Formaldehyde	10 g/L	10 g/L	10 g/L	DMAB	10 g/L	10 g/L	10 g/L
Thiourea	-	1 ppm	1 ppm	BTA	-	1 ppm	1 ppm
$KMnO_4$	-	-	1 ppm	MSA	-	-	1 ppm
NaOH (pH)	13.0	13.0	13.0	KOH (pH)	11.0	11.0	11.0
Temperature	60 °C	60 °C	60 °C	Temperature	30 °C	30 °C	30 °C

Table 2. Bath components and parameters of EDTA and xylitol contained autocatalytic plating baths.

Cyclic voltammetry (CV)

Three duplicates of each cyclic voltammetry (CV) measurement were made to guarantee repeatability. Copper deposition CV curves in commercial and environmentally friendly baths are shown in Fig. 4. Understanding the redox processes at the electrode surface is possible because of the distinct anodic and cathodic peaks that are seen. Around X V, the anodic peak represents the oxidation of Cu-to-Cu^{2+}, while around Y V, the cathodic peak represents the reduction of Cu^{2+} ions to metallic copper.

As the scan rate increases, the anodic peak potential shifts toward more negative values, indicating diffusion-controlled kinetics. Diffusion-limited electron transfer is characterized by Randles-Evčík behavior, which is further supported by the linear connection between peak current and the square root of the scan rate. In the presence of stabilizers such as thiourea and benzotriazole, suppression of the anodic oxidation current is evident, highlighting their inhibitory effect on uncontrolled copper dissolution. Conversely, partial oxidation of the stabilizer enhances deposition currents, consistent with stabilizer–metal ion interactions reported in earlier studies.

These electrochemical trends directly correlate with the surface morphologies observed in SEM and AFM analyses. Notably, the negative shift of the anodic peak also suggests improved electron-transfer kinetics and easier nucleation of copper. Higher stabilizer oxidation currents suppress copper deposition, whereas reduced stabilizer activity promotes enhanced deposition. Similar shifts in anodic potential have been documented in previous copper deposition studies, where stabilizer oxidation was shown to significantly influence nucleation density and film compactness.

Tafel polarization

The Tafel polarization curves (Fig. 5) reveal distinct electrochemical responses between EDTA- and xylitol-based baths. In the EDTA system, the plain bath (A) exhibited an Icorr of 37.6 µA cm^{-2}, which decreased to 22.6 µA cm^{-2} with the addition of thiourea (B) and further to 20.5 µA cm^{-2} upon incorporation of $KMnO_4$ (C).

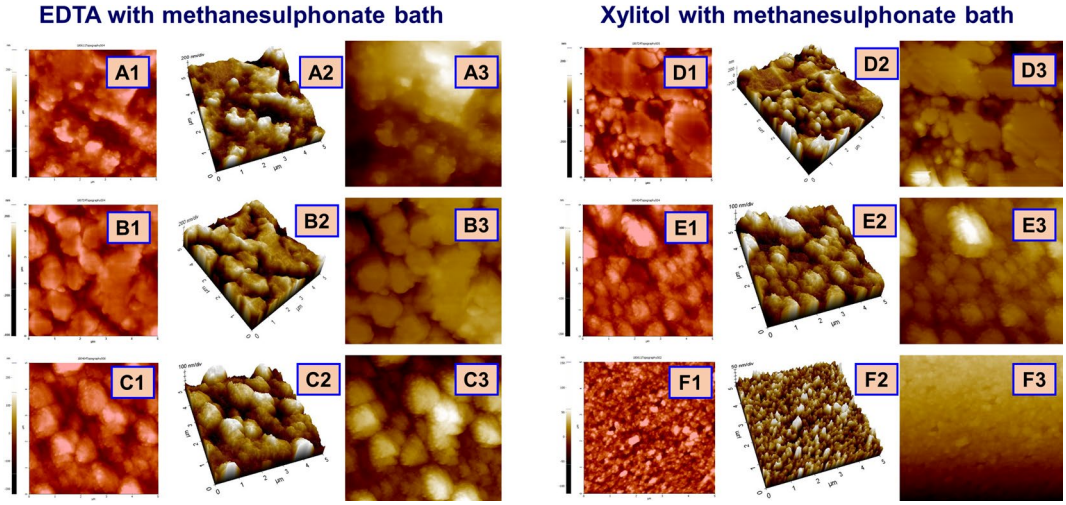

Fig. 3. AFM images of copper films obtained from EDTA and Xylitol contained methane sulphonate baths: (1) topography of copper deposits, (2) 3-D image, and (3) surface area. (**A**) EDTA standard bath, (**B**) EDTA standard bath with thiourea, (**C**) EDTA standard bath in thiourea, along with $KMnO_4$ (1 ppm), (**D**) xylitol standard bath, (**E**) xylitol standard bath with MSA and BTA (1 ppm), and (**F**) xylitol standard bath with MSA and BTA (1 ppm).

	Physical properties	Structural properties				Electrochemical properties					
									Charge transfer resistance (Rt) (mΩ/cm²)		
Bath contains	Deposition rate (μm/h)	Shapes	Roughness value (nm)	Crystallite size (nm)	Specific surface area (m^2/g)	E_{pa-1} values (V)	I_{pa-1} values (A)	I_{corr} (mA)	R_1	R_2	R_3
EDTA plain bath (A)	3.23	Needles	76.017	39.68	3.679	− 0.236	1.086×10^{-5}	37.6	7.47	5.32	82.28
EDTA plain bath + stabilizer (B)	2.72	Rocks	65.991	28.70	4.525	− 0.369	3.796×10^{-5}	22.6	13.9	10.83	78.54
EDTA plain bath + stabilizer + additives (C)	2.72	Pyramids	60.095	25.55	5.315	− 0.405	8.043×10^{-5}	20.5	11.24	11.04	67.86
Xylitol plain bath (D)	3.02	Coarse grain	49.583	24.07	7.787	− 0.2210	3.054×10^{-5}	50.64	5.46	4.82	52.48
Xylitol plain bath + stabilizer (E)	3.46	Small grain	38.798	20.17	9.301	− 0.167	4.395×10^{-5}	65.3	9.03	6.98	46.22
Xylitol plain bath + stabilizer + additives (F)	3.46	Flower	21.624	17.82	12.87	− 0.145	1.337×10^{-5}	75.3	4.23	4.49	28.27

Table 3. Physical, structural, electrochemical properties of EDTA and xylitol contained in methane sulphonate baths.

This progressive reduction in corrosion current, despite a slight decrease in deposition rate (3.23 to 2.72 μm h^{-1}), highlights the beneficial role of stabilizers and additives in producing more protective films. In contrast, the xylitol-based baths showed an opposite trend. The plain bath (D) started at 50.64 μA cm^{-2} using a coating process of 3.02 μm h^{-1}, the introduction of a stabilizer (E) raised Icorr to 65.3 μA cm^{-2}, and further addition of additives (F) increased it to 75.3 μA cm^{-2}, even though the deposition rate improved to 3.46 μm h^{-1}. These results indicate that, while xylitol formulations promote faster growth, they compromise film integrity and corrosion resistance when modified with stabilizers and additives. Overall, the comparison demonstrates that EDTA-based baths benefit from additive-induced inhibition, whereas xylitol-based baths trade protection for accelerated deposition.

Spectroscopy of electrochemical impedance (EIS)

An important source of information on the interfacial mechanisms controlling the corrosion resistance of copper deposits is electrochemical impedance spectroscopy (EIS) (Fig. 6). In Nyquist plots, the larger semicircle diameters observed for the eco-friendly xylitol–BTA bath compared with the EDTA system indicate significantly higher charge-transfer resistance, confirming the superior ability of these coatings to block electron transfer during corrosion. This reflects the formation of denser, more uniform barriers that effectively hinder chloride ion penetration.

Bode analysis further supports this trend. Xylitol-based coatings exhibit higher phase angles over a wide frequency range and greater impedance at low frequencies, features characteristic of capacitive, protective films. In contrast, EDTA-based coatings show lower phase angles and reduced impedance, signifying weaker barrier performance and susceptibility to localized breakdown. Equivalent circuit modelling reinforces these findings. Higher resistance values combined with lower constant phase element (CPE) values for eco-friendly

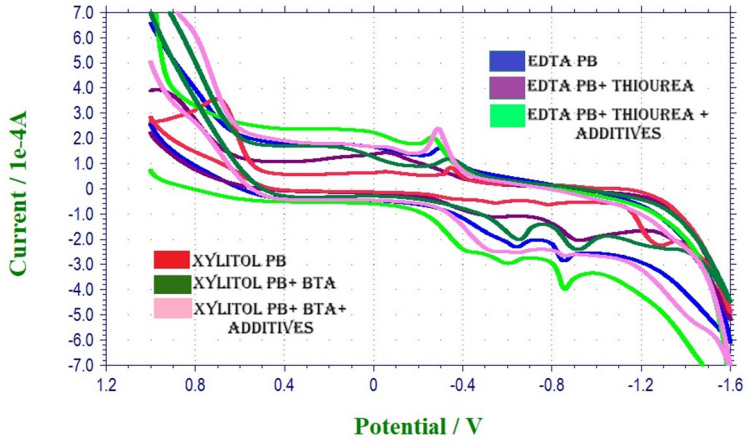

Fig. 4. Cyclic voltammetry (CV) curves for copper deposition in different electroless baths: (**A**) EDTA standard bath, (**B**) EDTA standard bath with thiourea, (**C**) EDTA standard bath in thiourea, along with $KMnO_4$ (1 ppm), (**D**) xylitol standard bath, (**E**) xylitol standard bath with MSA and BTA (1 ppm), and (**F**) xylitol standard bath with MSA and BTA (1 ppm).

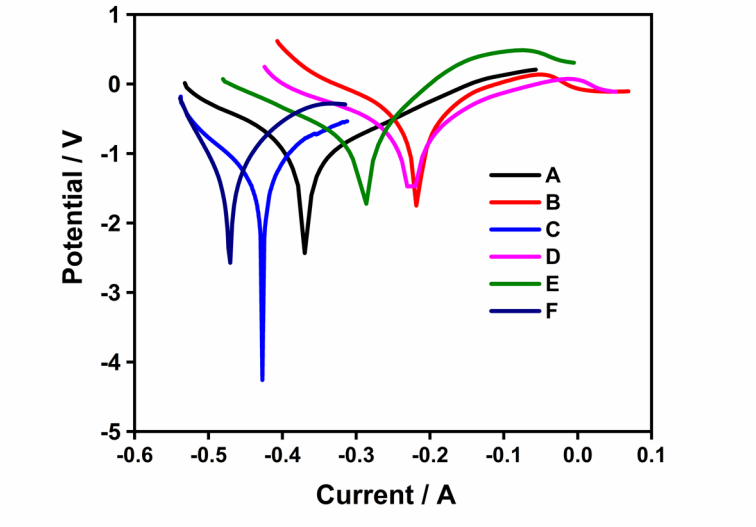

Fig. 5. Tafel polarization curves comparing corrosion behavior of deposits obtained from: (**A**) EDTA standard bath, (**B**) EDTA standard bath with thiourea, (**C**) EDTA standard bath in thiourea, along with $KMnO_4$ (1 ppm), (**D**) xylitol standard bath, (**E**) xylitol standard bath with MSA and BTA (1 ppm), and (**F**) xylitol standard bath with MSA and BTA (1 ppm).

coatings point to reduced double-layer capacitance, smoother interfaces, and fewer surface defects—consistent with AFM and SEM observations of compact, fine-grained morphologies. The role of stabilizers is also evident. Benzotriazole (BTA) enhances passivation and suppresses anodic dissolution, thereby improving film stability. Conversely, the EDTA–thiourea bath yields coatings with lower resistance and higher CPE values, reflecting porous microstructures and faster corrosion kinetics.

Overall, the EIS results establish a strong correlation between bath chemistry, electrochemical response, and film structure. The eco-friendly formulation consistently produces coatings with superior charge-transfer resistance, enhanced capacitive behavior, and stronger passivation—translating into markedly higher corrosion resistance and long-term durability compared with conventional EDTA-based systems.

The electrochemical analysis (CV, Tafel, and EIS) provides consistent evidence that eco-friendly electroless copper baths, particularly those containing xylitol and natural additives such as BTA, can achieve deposition performance comparable to or better than EDTA-based systems. Negative shifts in anodic potential, higher deposition rates, and larger impedance semicircle diameters collectively indicate improved nucleation, growth, and corrosion resistance in these baths. Compared with valuable conventional EDTA systems, xylitol-based

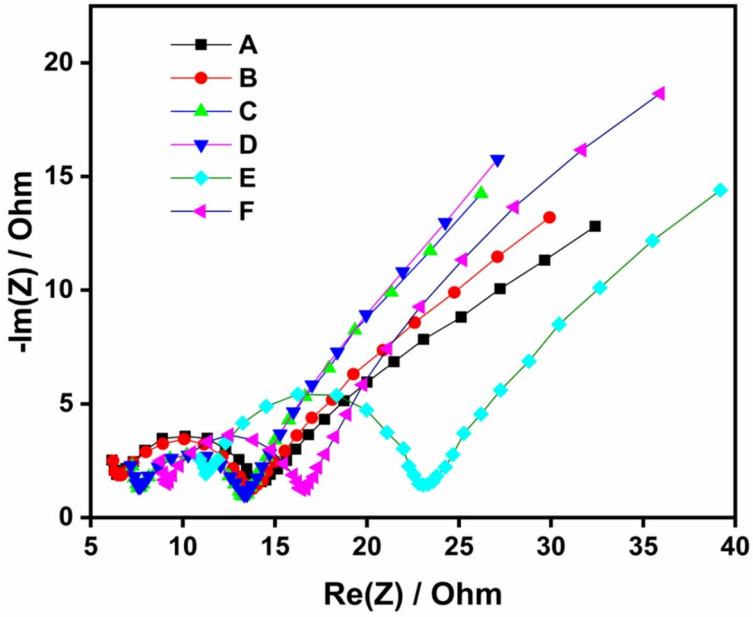

Fig. 6. Electrochemical impedance spectroscopy (EIS) results for copper coatings deposited from (**A**) EDTA standard bath, (**B**) EDTA standard bath with thiourea, (**C**) EDTA standard bath in thiourea, along with $KMnO_4$ (1 ppm), (**D**) xylitol standard bath, (**E**) xylitol standard bath with MSA and BTA (1 ppm), and (**F**) xylitol standard bath with MSA and BTA (1 ppm).

formulations show clear advantages in terms of stability and environmental compatibility. However, the present study is limited to laboratory-scale conditions, and further optimization is required before industrial application.

Conclusion

The following conclusions may be made following the successful application of copper film onto epoxy sheets utilizing two different electroless baths:

- This study highlights distinct performance differences between commercial EDTA-formaldehyde baths and eco-friendly formulations using biodegradable reducing agents and stabilizers. While conventional EDTA baths yield adherent, glossy copper coatings with good corrosion resistance and suitability for electronic applications, the deposits often display pyramidal or needle-like morphologies, with surface roughness exceeding 70 nm and larger crystallite sizes compared with eco-friendly alternatives.
- Formaldehyde, a component of EDTA baths, is corrosive to tracheal tissues, possesses high vapor pressure, and is carcinogenic. Moreover, EDTA is only weakly biodegradable. When combined with the pH adjuster, sodium hydroxide, byproducts such as succinic acid are formed. Additionally, this electroless bath prefers a higher alkaline medium at pH 13.0 and temperatures above 60 °C for stability.
- The second non-toxic (Xylitol) bath employs environmentally friendly organic substances. It is non-corrosive and biodegradable, providing excellent adherent coating, finer and smoother deposition, and broader coating applications, especially in marine equipment. Without appreciably changing the rate of deposition, novel additions like methane sulphonic acid support the enhancement of surface gloss in metallic copper. The BTA-filled bath acts as an accelerator.
- For coating purposes, xylitol, DMAB, and MSA are recognized as non-toxic and safe. When using KOH as a pH adjuster at a temperature of 30 °C, no accumulation, precipitation, or vapor pressure is formed. The resulting coating exhibits a uniform grain shape, roughness values below 50 nm, and is in good agreement with crystallite size. • In these active electroless baths, the electron density, steric hindrance, electron resonance, polarization effect, resonance effects, and the presence of heteroatoms (sulfur and nitrogen) in the complexing agents all have a significant impact on the surface morphologies of copper deposits.
- Overall, the superior morphology, lower corrosion currents, and higher impedance values of the eco-friendly bath are consistent with recent literature trends, confirming its potential as a reliable and sustainable alternative to EDTA-based commercial baths.

Data availability

The datasets used and/or analysed during the current study available from the corresponding author on reasonable request.

Received: 20 May 2025; Accepted: 8 September 2025
Published online: 29 September 2025

References

1. Guerra, L., Echeverría, F. & Correa, E. Effect of pH on dimethylamine borane reduced electroless nickel deposits on AISI/SAE 1045 steel surface. *Met. Mater. Int.* **26**, 773–782. https://doi.org/10.1007/s12540-019-00362-8 (2020).
2. Dev, S., Tandon, P., Jha, P., Singh, A. & Dutt Investigation of process parameters in electroless copper plating on polystyrene. *Sādhanā* **25**, 156. https://doi.org/10.1007/s12046-020-01377-3 (2020).
3. Chiang, C. H., Lin, C. C. & Hu, C. C. Effects of thiourea and allyl thiourea on the electrodeposition and microstructures of copper from methanesulfonic acid baths. *J. Electrochem. Soc.* **168**, 032505. https://doi.org/10.1149/1945-7111/abec56 (2021).
4. Azar, G. T. P., Fox, D., Fedutik, Y., Krishnan, L. & Cobley, A. J. Functionalized copper nanoparticle catalysts for electroless copper plating on textiles. *Surf. Coat. Technol.* **396**, 125971. https://doi.org/10.1016/j.surfcoat.2020.125971 (2020).
5. Muench, F. Electroless plating of metal nanomaterials. *ChemElectroChem* **8**, 2984–2984. https://doi.org/10.1002/celc.202100931 (2021).
6. Georgieva, M. G. Study of a system for creating a statistical model of the electroless plating of Cu-Ni-P alloys. *Trans. IMF.* **100**, 318–323. https://doi.org/10.1080/00202967.2022.2107773 (2022).
7. Sharifi, J., Paserin, V. & Fayazfar, H. Sustainable direct metallization of 3D-printed metal-infused polymer parts: a novel green approach to direct copper electroless plating. *Adv. Manuf.* **12**, 784–797. https://doi.org/10.1007/s40436-024-00486-0 (2024).
8. Abdulrhman, M., Zhakeyev, A., Fernández-Posada, C. M., Melchels, F. P. W. & Marques-Hueso, J. Routes towards manufacturing biodegradable electronics with Polycaprolactone (PCL) via direct light writing and electroless plating. *Flex. Print. Electron.* **7**, 025006. https://doi.org/10.1088/2058-8585/ac6b6e (2022).
9. Sood, Srishti, N. et al. Green and sustainable Pd-Co nanoparticle assisted electroless copper-plated cotton fabric for multifaceted catalytic and antimicrobial applications. *J. Clean. Prod.* **508**, 145495. https://doi.org/10.1016/j.jclepro.2025.145495 (2025).
10. Ratautas, K. et al. Evaluation and optimization of the SSAIL method for laser-assisted selective electroless copper deposition on dielectrics. *Results Phys.* **15**, 102943. https://doi.org/10.1016/j.rinp.2020.102943 (2020).
11. Zou, J., Shi, J., Yang, J., Li, J. & Liu, Y. Electroless copper plating mechanism of mesophase pitch-based carbon fibers by the grafting modification of silane coupling agents. *Mater. Today Commun.* **32**, 104053. https://doi.org/10.1016/j.mtcomm.2022.104053 (2022).
12. You, J. L. et al. Electroless plating of a 5G copper antenna on polyimide patterned with laser-induced selective activation and curing of metal–organic catalyst. *Appl. Surf. Sci.* **599**, 153990. https://doi.org/10.1016/j.apsusc.2022.153990 (2022).
13. Shin, B. K. et al. Microstructural and physicochemical origins of electroless copper deposition on graphite enhanced by acid pretreatment. *Mater. Chem. Phys.* **295**, 127118. https://doi.org/10.1016/j.matchemphys.2022.127118 (2023).
14. Luo, L. et al. Synthesis of carbon-based Ag-Pd bimetallic nanocomposite and the application in electroless copper deposition. *Electrochim. Acta.* **439**, 141679. https://doi.org/10.1016/j.electacta.2022.141679 (2023).
15. Bragaglia, M., Paleari, L., Mariani, M. & Nanni, F. Sustainable formaldehyde-free copper electroless plating on carbon-epoxy substrates. *J. Mater. Sci: Mater. Electron.* **35**, 707. https://doi.org/10.1007/s10854-024-12493-9 (2024).
16. Wang, P. et al. Selectively metalizable low-temperature cofired ceramic for three-dimensional electronics via hybrid additive manufacturing. *ACS Appl. Mater. Interfaces.* **14**, 28060–28073. https://doi.org/10.1021/acsami.2c03208 (2022).
17. Bian, Y. et al. Patterning techniques based on metallized electrospun nanofibers for advanced stretchable electronics. *Adv. Sci.* **11**, 2309735. https://doi.org/10.1002/advs.202309735 (2024).
18. Hui, W. Q. & Song, L. X. Study on a new process of electroless copper plating pretreatment on carbon fiber surface. *Mater. Res. Express.* **10**, 025604. https://doi.org/10.1088/2053-1591/acac02 (2023).
19. Fdo, S. A., Venkatesh, P. & BalaRamesh, P. Electroless copper deposition using 3-mercaptopropionic acid as an additive. *Mater. Today Proc.* **47**, 1883–1886. https://doi.org/10.1016/j.matpr.2021.03.583 (2021).
20. Chu, Z. et al. Magnetic, self-heating, and superhydrophobic sponge for solar-driven high-viscosity oil-water separation. *J. Hazard. Mater.* **445**, 130553. https://doi.org/10.1016/j.jhazmat.2022.130553 (2023).
21. Pawar, K. & Dixit, P. A critical review of copper electroless deposition on glass substrates for microsystems packaging applications. *Surf. Eng.* **38**, 576–617. https://doi.org/10.1080/02670844.2022.2142002 (2022).
22. Zhang, Y., Zhang, T., Shi, H., Liu, Q. & Wang, T. Fabrication of flexible copper patterns by electroless plating with copper nanoparticles as seeds. *Appl. Surf. Sci.* **547**, 149220. https://doi.org/10.1016/j.apsusc.2021.149220 (2021).
23. Lai, Z. et al. Cyanide-free silver immersion deposition involving 3-mercapto-1-propanesulfonic acid for copper finishing. *Mater. Chem. Phys.* **244**, 122671. https://doi.org/10.1016/j.matchemphys.2020.122671 (2020).
24. Rahman, U., Kabeb, S. M. & Zulfkifli, F. H. Functional hydrophobic coatings: insight into mechanisms and industrial applications. *Prog Org. Coat.* **203**, 109187. https://doi.org/10.1016/j.porgcoat.2025.109187 (2025).
25. Akin, S., Nath, C. & Jun, M. B. G. Selective surface metallization of 3D-printed polymers by cold-spray-assisted electroless deposition. *ACS Appl. Electron. Mater.* **5**, 5164–5175. https://doi.org/10.1021/acsaelm.3c00893 (2023).
26. Chen, L. & Su, R. K. L. Corrosion rate measurement by using the polarization resistance method for microcell and macrocell corrosion: theoretical analysis and experimental work with simulated concrete pore solution. *Constr. Build. Mater.* **267**, 121003. https://doi.org/10.1016/j.conbuildmat.2020.121003 (2021).
27. Gundry, L. et al. Recent advances and future perspectives for automated parameterization, bayesian inference, and machine learning in voltammetry. *Chem. Commun.* **57**, 1855–1870. https://doi.org/10.1039/d0cc07549c (2021).
28. Georgieva, M. et al. Electroless copper plating of dielectrics from environmentally friendly reducer-free electrolyte. *Trans. IMF.* **99**, 238–245. https://doi.org/10.1080/00202967.2021.1957339 (2021).
29. Tamayo, J. A., Ramírez-Sánchez, C. & Calderón, J. A. Effect of ammoniacal thiosulfate solution composition on the gold dissolution rate: an electrochemical study. *Electrochim. Acta.* **510**, 145359. https://doi.org/10.1016/j.electacta.2024.145359 (2025).
30. Jayalakshmi, S. et al. The effect of chelators on additives in the surface characterization and electrochemical properties of an eco-friendly electroless copper nanodeposition. *Sci. Rep.* **13**, 11062. https://doi.org/10.1038/s41598-023-38115-8 (2023).
31. Liu, C. et al. Copper deposit development potential on the Qinghai-Xizang plateau in China based on the pressure-state-response framework. *Sci. Rep.* **15**, 4589. https://doi.org/10.1038/s41598-025-89046-5 (2025).
32. Lazanas, C. & Prodromidis, M. I. Electrochemical impedance spectroscopy—A tutorial. *ACS Meas. Sci. Au.* **3**, 162–193. https://doi.org/10.1021/acsmeasuresciau.2c00070 (2023).

Acknowledgements

This work was supported by the National Research Foundation of Korea (NRF) grant funded by the Korea government (MSIT) (RS-2025-22222973).

Author contributions

Palanivelu Balaramesh: Formal analysis, Writing—original draft. Raja Venkatesan: Methodology, Investigation, Writing—original draft. Suseela Jayalakshmi: Investigation, Data curation. Munusamy Settu: Resources, Software. Eswaran Kamaraj: Conceptualization, Data curation, Writing—review and editing. Alexandre A. Vetcher: Investigation, Writing - original draft. Seong-Cheol Kim: Supervision, Project administration, Funding acquisition, Writing—review and editing. All authors have read and agreed to the published version of the manuscript.

Funding
This work was supported by the "2024 System Semiconductor Technology Development Program" funded by Chungbuk Technopark.

Declarations

Competing interests
The authors declare no competing interests.

Consent to participate
All person named as author in this manuscript have participated in the planning, design and performance of the research and in the interpretation of the result.

Consent for publication
All authors have indorsed the publication of this research.

Additional information
Correspondence and requests for materials should be addressed to R.V., M.S. or S.-C.K.